

# Fault diagnosis for fuel cell systems: A data-driven approach using high-precise voltage sensors

Zhongliang Li<sup>a,b,c,\*</sup>, Rachid Outbib<sup>a</sup>, Stefan Giurgea<sup>b,c</sup>, Daniel Hissel<sup>b,c</sup>,  
Alain Giraud<sup>d</sup>, Pascal Couderc<sup>e</sup>

<sup>a</sup>*Aix Marseille Univ, Universit de Toulon, CNRS, LIS, Marseille, France*

<sup>b</sup>*FCLAB (Fuel Cell Lab) Research Federation, FR CNRS 3539, rue Thierry Mieg, 90010 Belfort Cedex, France*

<sup>c</sup>*FEMTO-ST (UMR CNRS 6174), ENERGY Department, UFC/UTBM/ENSMM, France*

<sup>d</sup>*CEA/LIST, 91191 Gif-sur-Yvette Cedex, France*

<sup>e</sup>*3D PLUS, 78532 BUC, France*

---

## Abstract

Reliability and durability are two key hurdles that prevent the widespread use of fuel cell technology. Fault diagnosis, especially online fault diagnosis, has been considered as one of the crucial techniques to break through these two bottlenecks. Although a large number of works dedicated fuel cell diagnosis have been published, the criteria of diagnosis, especially online diagnosis have not yet been clarified. In this study, we firstly propose the criteria used for evaluating a diagnosis strategy. Based on that, we experimentally demonstrate an online fault diagnosis strategy designed for Proton Exchange Membrane Fuel Cell (PEMFC) systems. The diagnosis approach is designed based on advanced feature extraction and pattern classification techniques,

---

\*Corresponding author. Tel.: +33 (0)4 91 05 60 32, Fax: +33 (0)4 91 05 60 33. E-mail address: zhongliang.li@lisis.org (Z. LI), rachid.outbib@lisis.org (R. OUTBIB), stefan.giurgea@utbm.fr (S. GIURGEA), daniel.hissel@univ-fcomte.fr (D. HISSEL), alain.giraud@cea.fr (A. GIRAUD), pcouderc@3d-plus.com (P. COUDERC)

and realized by processing individual fuel cell voltage signals. We also develop a highly integrated electronic chip with multiplexing and high-speed computing capabilities to fulfill the precise measurement of multi-channel signals. Furthermore, we accomplish the diagnosis algorithm in real-time. The excellent performance in both diagnosis accuracy and speediness over multiple fuel cell systems is verified. The proposed strategy is promising to be utilized in various fuel cell systems and promote the commercialization of fuel cell technology.

*Keywords:* PEMFC system, Fault diagnosis, Application specific integrates circuit, Data-driven, Classification, Online implementation

---

## 1. Introduction

Fuel cell technology, because of its potential for effectively alleviating environmental and resource issues, has been attracting considerable increasing attention. Among the various fuel cells, proton exchange membrane fuel cell (PEMFC), thanks to its high power density and efficiency, low operating temperature, and quick response to load, is the most promising one to be widely applied in both stationary and automotive cases. However, reliability and durability are currently two main barriers which prevent the process for its wide applications [1, 2]. Among the solutions, fault diagnosis, more particularly online diagnosis, dedicated to detecting, isolating, and analyzing different faults, has proved to be beneficial for keeping fuel cell systems operating safely, reducing downtime and mitigating performance degradation [3, 4, 5].

The operation of a PEMFC system involves multiple auxiliary subsystems

15 other than fuel cell stack, and requires multi-field knowledge, for example  
16 complex electrochemistry, thermodynamics, and fluid mechanics. To accu-  
17 rately detect and identify the faults occurring in the system is not a trivial  
18 task. During the last decade, considerable attention has been focused on the  
19 topics related to fault diagnosis for PEMFC systems.

20 Among the most substantial approaches, model based fault diagnosis ap-  
21 proaches have been proposed. A review of model based methods is available  
22 in [6]. Most of these approaches are based on some general input-output  
23 or state space models, which are usually developed from the physical and  
24 mathematical knowledge of the process [7]. In [8], the authors developed  
25 an electrical equivalent circuit which can be seen as an analytical model of  
26 the concerned PEMFC system. The component parameters are identified  
27 and the variation of the specific electrical component values can be seen as  
28 the indicator of the corresponding faults. In [9], a linear parameter vary-  
29 ing (LPV) model is built for a commercial PEMFC system. An observer  
30 is proposed based on the proposed LPV model. Then, the residuals can  
31 be computed by comparing the process outputs and the outputs estimated  
32 from the observer. The similar methods are also used in [10, 11]. Besides  
33 designing a specific observer, the parity relation is also used for residual  
34 generation procedure in a more straightforward way [12]. To carry out the  
35 above mentioned three kinds of analytical model based approaches, an accu-  
36 rate process model of PEMFC systems is necessary. However, modeling the  
37 PEMFC systems is a rather difficult task. Especially, the identification of  
38 fuel cell inner parameters concerning the operation, the geometries as well  
39 as the materials is difficult [13]. Even the parameters are identified, some of

40 them are time-varying because of the ageing degradation. In addition, the  
41 existing models are usually not able to fulfill sufficient accuracy, generaliza-  
42 tion and real-time implementability, which makes model based approaches  
43 insufficiently suitable for wide practical applications [14].

44 Another branch named data-driven diagnosis has been gaining increasing  
45 attention. The data-driven methods are those make use of the information  
46 from the historical data other than an analytical model. A review of data-  
47 driven methods is available in [4]. In [15], [16], and [17], fuzzy inference and  
48 neural networks are used to build “black-box” models whose parameters are  
49 obtained by fitting the experimental data obtained in fault free state. With  
50 these “black-box” models, the diagnosis can be realized by evaluating the  
51 difference between the real system outputs and the model outputs. In [18], a  
52 multivariate analysis technique, named principal component analysis (PCA),  
53 is used for diagnosis by analyzing the variables measured by multiple sensors  
54 installed in a PEMFC system. In [19], the fuzzy clustering method is used to  
55 process the signals acquired from a commercial PEMFC system in order to  
56 achieve fault diagnosis. In [20] and [21], Bayesian networks classification is  
57 used for the PEMFC diagnosis. In [22], [23], and [24], the signal processing  
58 methods, fast fourier transform, wavelet transformation, multifractal formal-  
59 ism, are respectively used to extract the features which are sensitive to faults  
60 from the fuel cell stack voltage signals. Although some interesting prelimi-  
61 nary results have been proposed in the frame of data-driven diagnosis, the  
62 online validation of those approaches in different real PEMFC systems has  
63 not yet been announced.

64 Actually, some criteria have to be satisfied to realize online diagnosis for

65 PEMFC systems serving in real conditions. First, the sensors for measuring  
66 the variables serving as the inputs of the fault diagnosis approach should be  
67 minimized and arranged in limited space. The intrusive and/or costly sensors  
68 or instruments should be avoided whenever possible. Second, the diagnosis  
69 accuracy should be maintained at a high level with respect to different faults  
70 and different PEMFC systems. Third, the online diagnosis approach needs  
71 to be computationally efficient since it is usually implemented in some “on-  
72 board” embedded system with limited computational power available [25, 26].  
73 Fourth, because of ageing effects, fuel cells’ behaviors are time-variant. The  
74 diagnosis approach should be capable of being adapted online. In addition,  
75 the serial-connected single fuel cells which compose a fuel cell stack are usu-  
76 ally considered to be identical in the existing approaches. Nevertheless, the  
77 inhomogeneity among cells should be more emphasized when we talk about  
78 “faults”. This is because usually a proportion of fuel cells fall into faulty  
79 state first when a fault occurs [27, 28].

80 In this article, we propose and experimentally demonstrate an online fault  
81 diagnosis strategy for PEMFC systems. To achieve the diagnosis goal, we de-  
82 signed an reduced volume application specific integrates circuit (ASIC) which  
83 integrate multichannel voltage sensors of giant magneto resistance (GMR)  
84 type, and a field programmable gate array (FPGA) based computing unit  
85 [29, 30]. The individual fuel cell voltages can be precisely measured and  
86 treated as the input variables of the diagnosis approach. The discriminant  
87 features are extracted using fisher discriminative analysis (FDA) from the  
88 vectors composed by cell voltages and classified the features using support  
89 vector machine (SVM) into different classes that represent different states of

90 health. Besides the requirements for a basic diagnosis approach, the novel  
91 fault detection and online adaptation functions are also developed and added  
92 to the proposed approach. They are realized through using specifically de-  
93 signed diagnosis rules and an incremental learning method. We verified the  
94 efficiency of our strategy via the experiments on several stacks and multiple  
95 faulty types. To our knowledge, this work is the first to provide a high-  
96 performance online diagnosis strategy implemented in an ASIC for PEMFC  
97 systems.

98 The rest of the paper is organized as follows: the development process of  
99 the proposed diagnosis strategy is given in Section 2. Section 3 and Section 4  
100 present respectively the diagnosis approach and the ASIC designed to realize  
101 diagnosis function. Experimental platform and database preparation are  
102 described in Section 5. Diagnosis results are summarized and analyzed in  
103 Section 6. We finally conclude the work in Section 7.

## 104 **2. Diagnosis strategy development process**

105 The proposed data-driven diagnosis strategy consists of offline and online  
106 stages (see Fig. 1(a)). The feature extraction (FDA) and the classification  
107 models (SVM) are trained and tested offline. The objective of the test stage  
108 is to optimize the parameters used for SVM. The trained models are imple-  
109 mented online to achieve the diagnosis goal. Moreover, based on the data  
110 sampled online, the SVM model can be adapted online.

111 The realization process is shown in Fig. 1(b). In the offline stage, the  
112 historical data (individual cell voltages) are measured using the GMR sensors  
113 integrated in the ASIC and saved as the training and test database into a

114 PC. Then the diagnosis model is trained using the PC and programmed into  
115 the memory of the ASIC. In the online stage, the variables (individual cell  
116 voltages) are measured and processed using the ASIC with the model trained  
117 offline.

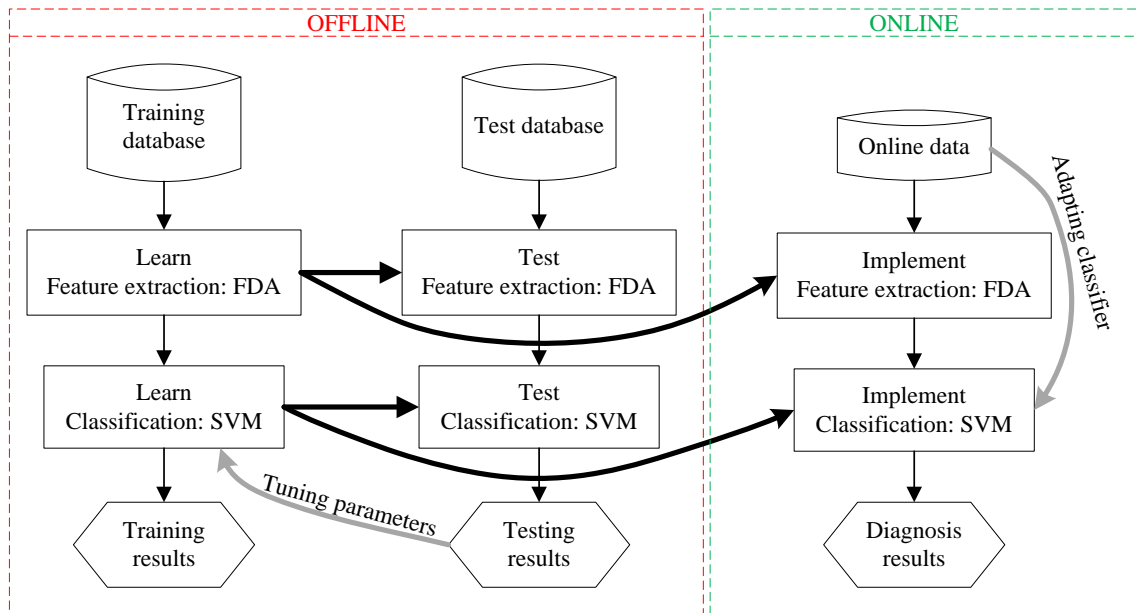
### 118 **3. Diagnosis approach**

119 In this section, the diagnosis problem and the involved methodologies are  
120 presented mathematically in a general manner. Actually, the main focus of  
121 this paper is to provide the completed implementation process of the pro-  
122 posed diagnosis strategy, which includes both software and hardware devel-  
123 opments. The mathematical details of the involved algorithms are provided  
124 by citing several published works.

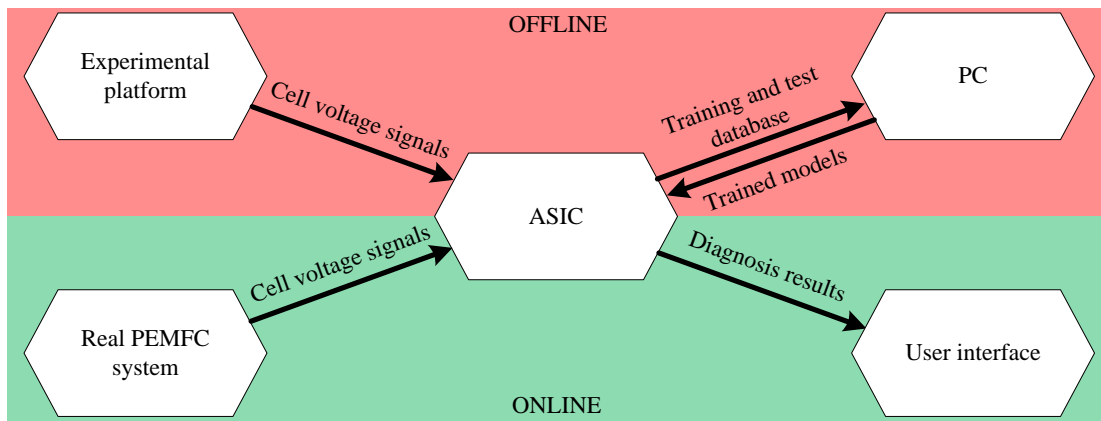
#### 125 *3.1. Problem formulation*

126 The diagnosis approach proposed in this study belongs to the category of  
127 supervised methods. The basic tasks of fault diagnosis, i.e. fault detection  
128 and isolation, can be abstracted as a typical pattern classification problem  
129 (see Fig. 2).

130 Suppose that the fuel cell stack in a concerned system is composed of  $M$   
131 single fuel cells. At a certain time, the individual cell voltages are measured  
132 and denoted as a vector  $\mathbf{v} = [v_1, v_2, \dots, v_M]^T$ . Suppose that we have a training  
133 dataset  $\mathbf{V}$  which consists of  $N$  such vectors, i.e.  $\mathbf{V} = \{\mathbf{v}_1, \mathbf{v}_2, \dots, \mathbf{v}_N\}$ . These  
134 vectors are known to be distributed in the classes denoted as  $\Omega_0, \Omega_1, \Omega_2, \dots,$   
135  $\Omega_C$ , in which the class label 0 corresponds to the fault free state, while 1, 2,  
136  $\dots, C$  correspond to the faults of various types. The class label  $g_i$  of vector  
137  $\mathbf{v}_i$  is known in prior. Based on the dataset  $\mathbf{V}$ , a function denoted as  $F(\cdot)$



(a)



(b)

Figure 1. Diagram of the proposed diagnosis approach and of the realization process. (a) Workflow of the proposed diagnosis approach. (b) Realization process of the diagnosis strategy.



138 can be trained offline. Through the function, the class label of a given vector  
 139 formed by the cell voltages can be determined as

$$g_n = F(\mathbf{v}_n) \quad (1)$$

140 The diagnosis procedure is the process of implementing this function online.

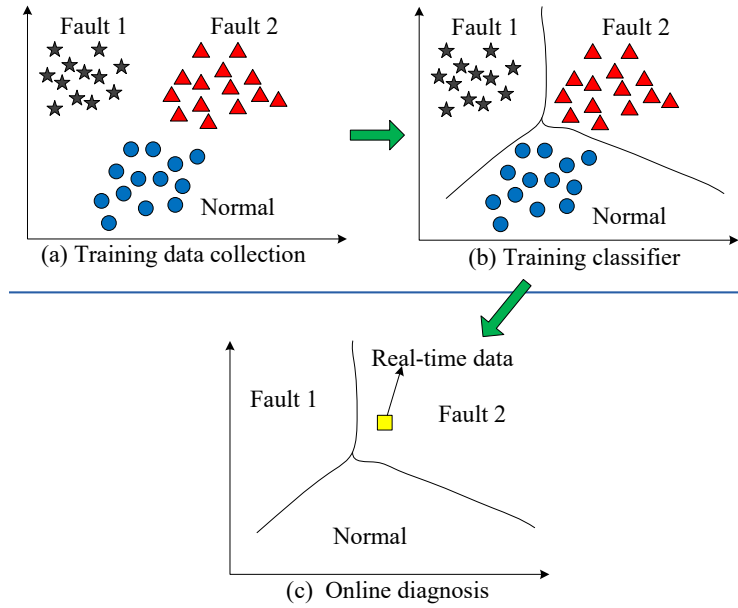


Figure 2. Principle of classification based fault diagnosis. The implementation of the approach can be divided into three steps. (a) The historical data in both health state and concerned faulty states are collected as the training data base. In this case, the data are distributed in three classes: normal, fault 1 and fault 2. (b) A classifier is trained based on the training data base. The trained classifier is described as the boundaries among the classes. (c) The trained classifier is performed online. According to the classifier or the boundaries here, an arbitrary online sample is classified into one of the concerned classes. Fault detection and isolation is thus realized. In this case, the online sample is classified into fault 2 class.

141 A large dimensional number  $M$ , i.e. the single fuel cell number, may

142 cause a heavy burden of online computation and a reduced diagnosis power.  
 143 We therefore propose a two-step diagnosis procedure to solve the problem as  
 144 follows: a feature extraction stage to reduce the original data dimensional  
 145 number is carried out first, as

$$\mathbf{z}_n = f_1(\mathbf{v}_n) \quad (2)$$

146 where  $\mathbf{z}_n$  is a  $L$ -dimensional vector composed of features ( $L < M$ ). Then,  
 147 the classification is implemented in the feature space as

$$g_n = f_2(\mathbf{z}_n) \quad (3)$$

148 Such that the diagnosis procedure is transformed into a two-step proce-  
 149 dure. By comparing several representative feature extraction and classifica-  
 150 tion methods from the point of view of diagnosis precision and computational  
 151 complexity, FDA and SVM methods were selected as the feature extraction  
 152 and classification tools, respectively [31].

### 153 3.2. Principle of FDA

154 FDA is a supervised technique developed to extract the features from the  
 155 data in the hope of obtaining a more manageable classification problem [32].  
 156 The objective of FDA is to project the data into a lower dimensional space  
 157 in which the variance between classes is maximized while the variance within  
 158 an identical class is minimized. Through the training process,  $C$  projecting  
 159 vectors ( $C$  fault types in the training dataset), denoted as  $\mathbf{w}_1, \mathbf{w}_2, \dots, \mathbf{w}_C$ ,  
 160 can be determined in the offline training phase. The features of the vector  
 161  $\mathbf{v}_n$  can be computed as  $\mathbf{z}_n = [\mathbf{w}_1^T \mathbf{v}_n, \mathbf{w}_2^T \mathbf{v}_n, \dots, \mathbf{w}_C^T \mathbf{v}_n]^T$ . The details on FDA  
 162 implementation can be found in [31].

163 *3.3. Principle of SVM*

164 SVM is a classification method developed originally by V. Vapnik in 1998  
165 and has been considered as the present state of art classifier [33]. SVM func-  
166 tions by projecting the data into a high-dimensional space and constructing  
167 a hyperplane which separates the cases of different classes in this space.  
168 Different from the basic SVM, spherical shaped multi-class support vector  
169 machine (SSM-SVM), considered as a modified version, was employed in our  
170 approach [34]. The principle of SSM-SVM is to project the original data  
171 into a high-dimensional space and seek multiple class-specific spheres which  
172 enclose the samples from an identical class while excluding those from the  
173 other classes in this space (see Fig. 3). The projection from original space to  
174 high-dimensional space and some data processing are realized by introducing  
175 a kernel function and playing “kernel trick”. Training a SVM classifier can be  
176 finally abstracted as a quadric problem, while implementing a SVM classifier  
177 involves a small proportion of the training data which are named “support  
178 vectors”.

179 To determine the class label of a sample  $\mathbf{z}_n$ , the following criterion is used

$$g_n = \arg \max_i G_i(d_i(\mathbf{z}_n)) \quad i = 0, 1, 2, \dots, C \quad (4)$$

180 where  $G_i$  is a smooth monotonous decreasing function,  $d_i(\mathbf{z}_n)$  is the distance  
181 from  $\mathbf{z}_n$  to the  $i$ th sphere center and it can be calculated based on training  
182 result. See [14] for more details of SSM-SVM classification.

183 *3.4. Diagnosis rules*

184 A conventional classification method can only classify a sample into a  
185 known class. It will lose its efficiency as a sample comes from a novel class,

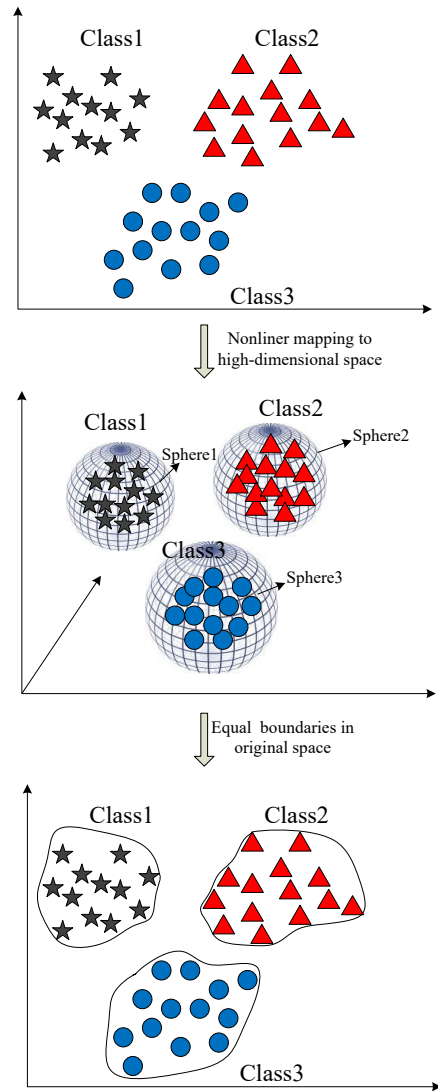


Figure 3. Principle of SSM-SVM classification. The training data are distributed in three classes labeled by class 1, class 2 and class 3. Through nonlinear mapping, the original data are projected into high-dimensional space (3-dimension in this case). In the high-dimensional space, the class-specific spheres can be found through training. The class-specific spheres enclose the samples from a specific class, while excluding those from the other classes. These spheres can be seen as the class-specific boundaries in the original space.

186 i.e. a novel faulty mode in our case. In order to recognize the novel faulty  
 187 mode, we propose to set boundaries for the spheres in high-dimension space.  
 188 The samples from a novel cluster can thus be detected if they are outside all  
 189 the closed boundaries. To realize this, the function  $G_i$  in terms of  $d_i(\mathbf{z})$  is  
 190 defined as

$$G_i(d_i(\mathbf{z})) = \begin{cases} 0.5 \left( \frac{1 - d_i(\mathbf{z})/R_i}{1 + \zeta_1 d_i(\mathbf{z})/R_i} \right) + 0.5 & \text{if } d_i(\mathbf{z}) \leq R_i \\ 0.5 \left( \frac{1}{1 + \zeta_2(d_i(\mathbf{z}) - R_i)} \right) & \text{otherwise} \end{cases} \quad (5)$$

191 where  $R_i$  is the radius of  $i$ th sphere,  $\zeta_1$  and  $\zeta_2$  are constants that satisfy  
 192  $R_i \zeta_2(1 + \zeta_1) = 1$ . It could be proved that  $G_i : \mathbb{R}_+ \rightarrow \mathbb{R}_+$  is a smooth  
 193 decreasing function with  $\lim_{\tau \rightarrow \infty} G_i(\tau) = 0$ .

194 It is considered that a sample  $\mathbf{z}$  belongs more probably to the class with  
 195 the shortest distance from the sphere center to the sample. However, if this  
 196 distance is still larger than a threshold, we will consider the sample is from  
 197 a novel class (novel fault mode). Mathematically, the diagnosis rule is

$$g_n = \begin{cases} \arg \max_i G_i(d_i(\mathbf{z})) & \text{if } \max_i G_i(d_i(\mathbf{z})) \geq \delta_i \\ \text{new} & \text{if } \max_i G_i(d_i(\mathbf{z})) < \delta_i \end{cases} \quad (6)$$

198 where the threshold  $\delta_i$  is determined based on a calibration dataset with  $N_i$   
 199 elements, and a way to fix its value is to use the *3-sigma law*:

$$\delta_i = M_i - 3 \sqrt{\frac{1}{N_i} \sum_{g_n=i} (G_i(d_i(\mathbf{z})) - M_i)^2} \quad (7)$$

200 with  $M_i = \frac{1}{N_i} \sum_{g_n=i} G_i(d_i(\mathbf{z}_n))$ .

### 201 3.5. Online adaptation method

202 Traditional SVM training is performed in one data batch and it must  
 203 be redone from scratch if the training dataset varies. The computational

204 cost for the training procedure is usually heavy and realized offline. To  
205 realize online updating of the classifier as time goes on, we propose here an  
206 incremental learning method for training the proposed SSM-SVM [14]. In  
207 this method, the solution for  $N+1$  training data could be formulated in terms  
208 of the solution for  $N$  data and one new data point. The light computational  
209 complexity makes the incremental learning procedure suitable for online use.  
210 The theoretical deduction of incremental learning can be found in [14].

#### 211 **4. ASIC developed for implementing the diagnosis approach**

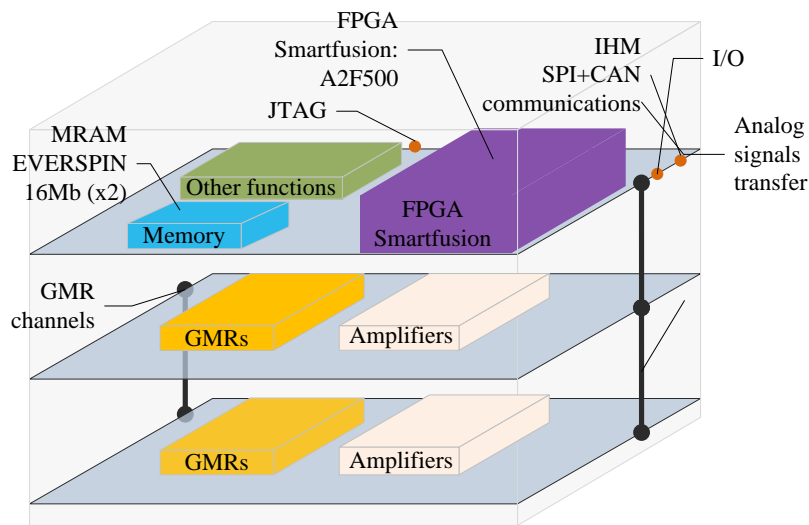
212 Since the input variables for the diagnosis approach we propose are in-  
213 dividual cell voltages, a sensor capable of precisely measuring the voltage  
214 signals of low amplitude and multiplexing is required. We propose here an  
215 integrated voltage sensor which is based on GMR technology [29]. Compared  
216 with the traditional Hall effect sensors which are commonly used for voltage  
217 or current measurement, the GMR sensors exhibit a much higher sensitivity  
218 especially in low current (voltage), high precision applications [35]. Knowing  
219 that a single cell voltage is usually less than 1 V, GMR sensors are well suited  
220 in our case. Moreover, the sensor developed here also improves the present  
221 state of the art in the aspects of increasing insulation capability ( $> 2000kV$ )  
222 [36].

223 To implement the proposed diagnosis approach, multiple GMR voltage  
224 sensors are packaged with a commercial system on chip (SoC) FPGA device  
225 which functions as the computation and communication unit. As shown in  
226 Fig. 4(a), these components are designed in the form of a 3D integration cir-  
227 cuit. The upper layer taking charge of computation and communication can

228 be seen as the “main board”. In this layer, the Smartfusion on-chip system  
229 developed by Microsemi is integrated. The device integrates an FPGA fab-  
230 ric, an ARM Cortex-M3 Processor, and programmable analog circuitry. The  
231 ARM Cortex-M3 processor is an 100 MHz, 32-bit CPU. The programmable  
232 analog circuitry can function as the D/A and A/D conversion blocks. This  
233 integrated device is equipped with up to 512 KB flash and 64 KB of SRAM.  
234 Besides, another two 16 M memory chips is added to the system. With the  
235 abundant connecting ports, different kinds of communications can be realized  
236 with other devices. The other two layers, which are equipped with GMR sen-  
237 sors, are adapted for measuring multi-channel voltage signals precisely. The  
238 appearance of the 3D ASIC and the test board are shown respectively in Fig.  
239 4(b) and Fig. 4(c).

## 240 5. Database preparation

241 In order to generate the database for training and testing the diagnosis  
242 model as well as validating the performance of online implementation, we  
243 carried out a series of experiments including the ones under normal operating  
244 condition and faulty conditions. The faults created deliberately cover the  
245 abnormal operations in different components of a PEMFC system, such as  
246 the water management subsystem, the temperature management subsystem,  
247 the electric circuit, the air and hydrogen circuits. The faults studied are  
248 usually considered as “reversible” or “recoverable”, which means they can be  
249 corrected through appropriate operations and do not cause the permanent  
250 defects in the systems. Actually, accurate diagnosis of this kind of faults can  
251 usually avoid the occurrence of those so-called permanent faults. During the



(a)



(b)



(c)

Figure 4. ASIC designed for monitoring individual fuel cell voltages and implementing the diagnosis approach. (a) The architecture of the ASIC, which was specially designed for the PEMFC system diagnosis. (b) The appearance of the designed ASIC. The ASIC is with compact package dimensions of  $27 \times 27 \times 12 \text{ mm}^3$ . (c) The ASIC is installed into a printed circuit board (PCB) which is equipped with the connectors, test points and LED lights.



252 experiments the data were captured using the designed ASIC and saved into  
253 the disk of a PC.

### 254 *5.1. PEMFC platform*

255 A 1 kW and a 10 kW experimental platform, which had been developed  
256 in-lab, were employed to fulfill the experimental requirements (see Fig. 5).  
257 In the hydrogen and air circuits, the temperatures, pressures, flow rates, and  
258 relative humidifies can be regulated in a wide range. A thermal-regulated  
259 water circuit ensures the flexible control of the stack temperature. The load  
260 current profile can be defined or simulated with the help of a DC electronic  
261 load. A terminal is installed into the stack to facilitate the connection to the  
262 ASIC and to monitor the cell voltages.

263 The platform enables us to emulate different faults artificially, and thus  
264 generate the database for both offline training and online validation. In or-  
265 der to verify the generalization performance of the proposed approach, three  
266 stacks from different industrial suppliers and with different cell numbers,  
267 power levels, mechanical designs were explored respectively on the two plat-  
268 forms (Fig. 6).

### 269 *5.2. Concerned faults*

270 Thanks to the home-made platforms in which a number of operating  
271 parameters can be set flexibly, we experimentally simulated a variety of faults  
272 that can potentially occur in different components of a PEMFC system.  
273 In order to cover the possible fault types, 7 fault types involving different  
274 subsystems or components were explored in this study. These faults and  
275 corresponding operations are summarized in Table 3. In addition to the

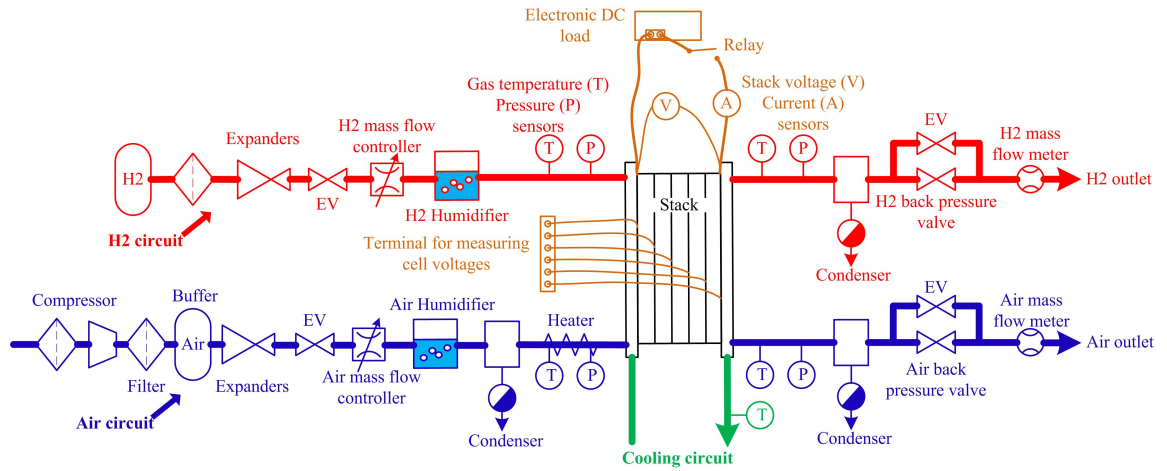


Figure 5. Schematic of the platforms used for generating the training and test database and for online validation.

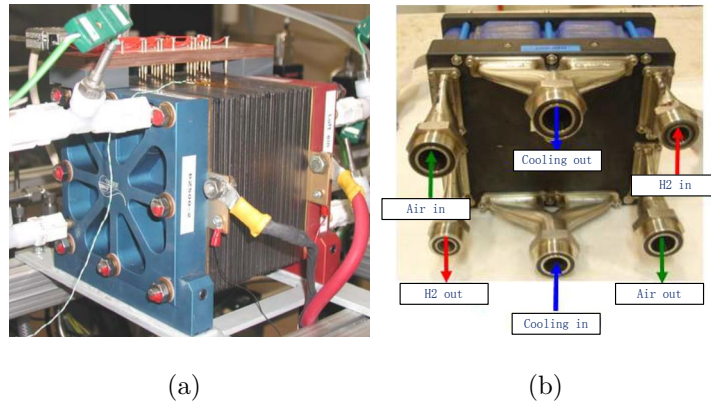


Figure 6. (a) 20-cell stack installed in the platform. (b) Appearance of the 8-cell stack and 40-cell stack.

Table 1. Technical parameters of the 20-cell stack

| Parameter                    | Value               |
|------------------------------|---------------------|
| Active area                  | 100 cm <sup>2</sup> |
| Flow field structure         | serpentine          |
| Electrode surface area       | 100 cm <sup>2</sup> |
| Nominal output power         | 500 W               |
| Operating temperature region | 20-65 °C            |
| Maximum operating pressures  | 1.5 bar             |
| Anode stoichiometry          | 2                   |
| Cathode stoichiometry        | 4                   |

276 individual cell voltages, a detailed measurements of temperatures, current,  
 277 pressures and gas flow rates have been achieved thanks to the well-equipped  
 278 platforms. In this study, the importance is put on the combination of ASIC  
 279 and data-driven diagnosis approach and their implementation for various fuel  
 280 cell stacks. The detailed waveforms and analysis of the acquired data during  
 281 each fault experiment have been summarized in the previous articles [37] [28]  
 282 [38].

## 283 6. Results

284 We carried out a number of experiments in both normal operating and  
 285 faulty cases to collect the data for training and testing the proposed diagnosis  
 286 model. Then, the trained diagnosis model was programmed into the memory  
 287 of the ASIC and implemented online.

Table 2. Technical parameters of the 8-cell stack and 40-cell stack

| Parameter                                       | Value               |
|---|---------------------|
| Active area                                     | 200 cm <sup>2</sup> |
| Stoichiometry $H_2$                             | 1.5                 |
| Stoichiometry <i>Air</i>                        | 2                   |
| Pressure at $H_2$ inlet                         | 150 kPa             |
| Pressure at <i>Air</i> inlet                    | 150 kPa             |
| Pressure differential between anode and cathode | 30 kPa              |
| Temperature (exit of cooling circuit)           | 80 °C               |
| Anode relative humidity                         | 50%                 |
| Cathode relative humidity                       | 50%                 |
| Current   | 110 A               |
| Voltage per cell                                | 0.7 V               |
| Electrical power of 8-cell stack                | 616 W               |
| Electrical power of 40-cell stack               | 3080 W              |

Table 3. Experiments on various health states carried out on different PEMFC stacks

| Stack         | Health state description | Location                   | Operation                                       | Notation      |
|---------------|--------------------------|----------------------------|---|---------------|
| 20-cell stack | Normal operating         | Whole system               | Nominal operation                               | <i>Normal</i> |
|               | Flooding                 | Water management subsystem | Increase air relative humidity                  | $F_1$         |
|               | Membrane drying          | Water management subsystem | Deactivate air humidifier                       | $F_2$         |
| 8-cell stack  | Normal operating         | Whole system               | Nominal operation                               | <i>Normal</i> |
|               | High current pulse       | Electric circuit           | Short circuit                                   | $F_3$         |
|               | High temperature         | Temperature subsystem      | Stop cooling water                              | $F_4$         |
|               | High air stoichiometry   | Air supply subsystem       | Increase air stoichiometry to 2.0 normal value  | $F_5$         |
|               | Low air stoichiometry    | Air supply subsystem       | Decrease air stoichiometry to 0.6 normal value  | $F_6$         |
|               | Anode CO poisoning       | $H_2$ supply subsystem     | Feed hydrogen with 10 ppm CO                    | $F_7$         |
| 40-cell stack | Normal operating         | Whole system               | Nominal operation                               | <i>Normal</i> |
|               | High current pulse       | Electric circuit           | Short circuit                                   | $F_3$         |
|               | High temperature         | Temperature subsystem      | Stop cooling water                              | $F_4$         |
|               | High air stoichiometry   | Air supply subsystem       | Increase air stoichiometry to 2.2 normal value  | $F_5$         |
|               | Low air stoichiometry    | Air supply subsystem       | Decrease air stoichiometry to 0.65 normal value | $F_6$         |

288 As the individual cell voltages were used as the variables for diagnosis,  
289 the dimensional number of the original data was equal to the cell number in  
290 the concerned stack. By using the FDA method, the features were extracted  
291 from the original data. A part of extracted features are shown in Fig. 7(a),  
292 Fig. 7(b) and Fig. 7(c). From these figures, it can be seen that the features in  
293 normal state and different faulty states are generally separated in the lower  
294 dimensional feature space. The characteristic lightens the computational  
295 burden and improves the performance of the classification following feature  
296 extraction step [37].

297 In a diagnosis cycle, classification is conducted in the feature space follow-  
298 ing the feature extraction procedure. SSM-SVM, combined with the diagnos-  
299 tic rule, is implemented in this phase. To construct the SSM-SVM classifier,  
300 the radial basis function (RBF) was selected as the “kernel function”, and  
301 parameters including the penalty factor and kernel parameter were optimized  
302 based on the test database.

### 303 *6.1. Diagnosis accuracy*

304 We evaluated the online implementation results using two criteria: false  
305 alarm rate (FAR) which is the rate of the samples in normal state wrongly  
306 diagnosed into the faulty classes, and the diagnosis accuracy of each specific  
307 fault type. According to the recorded diagnosed results, FAR reaches respec-  
308 tively 2.82%, 0%, 2.09% for the three stacks, which exhibits a low level. The  
309 diagnosis accuracies of the 7 fault types concerned are listed in Table 4. It  
310 should be noted that the parameters are maintained at a high level ( $> 95\%$ )  
311 for most fault types ( $F_1, F_2, F_4, F_5, F_7$ ). The mis-classifications happened  
312 mostly on the data in  $F_6$  (low air stoichiometry fault) state, in which the cell

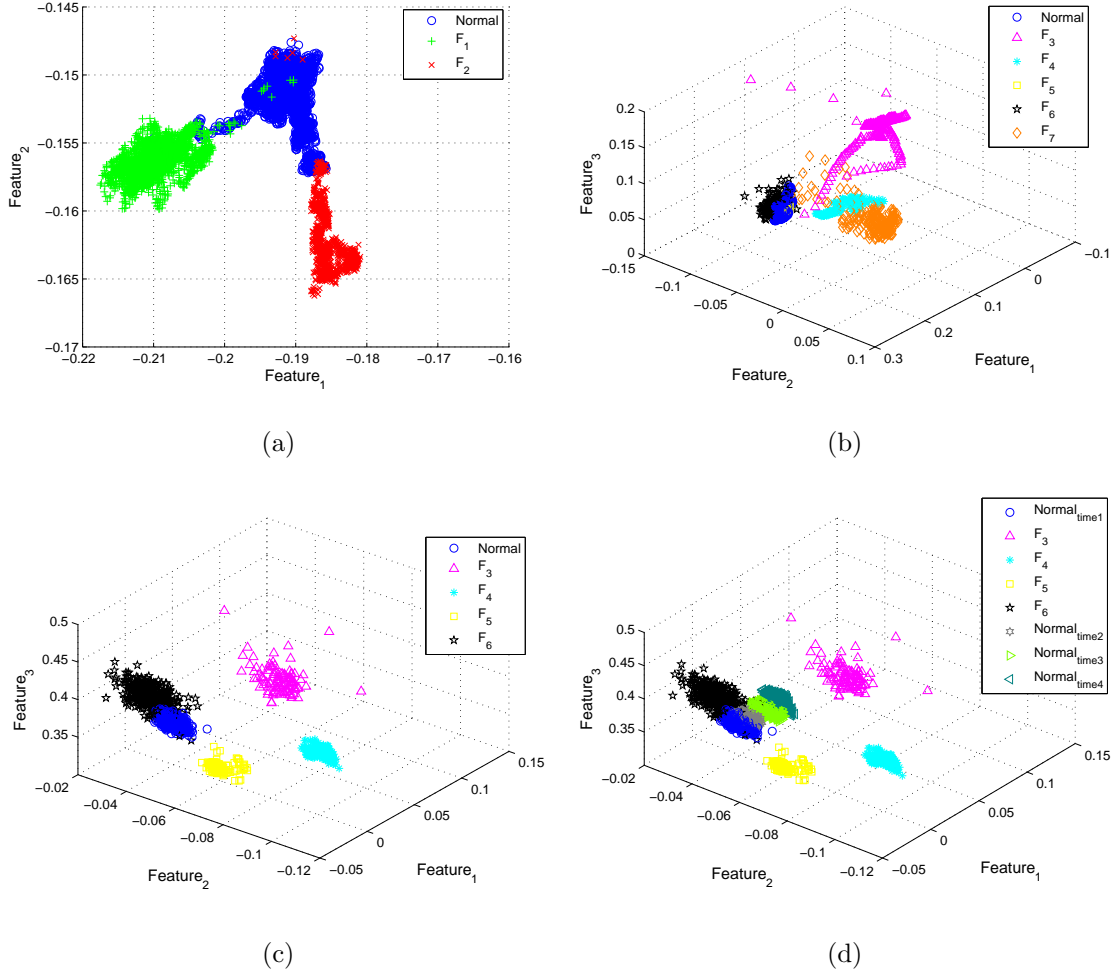


Figure 7. Features extracted from data of cell voltages. Normal,  $F_1$ ,  $F_2$ ,  $F_3$ ,  $F_4$ ,  $F_5$ ,  $F_6$  and  $F_7$  represent respectively the normal state, membrane drying fault, flooding fault, high current pulse fault, cooling water stopping fault, high air stoichiometry, low air stoichiometry, and anode CO poisoning. (a) 2-dimensional features extracted from the data in normal,  $F_1$  and  $F_2$  faulty states for a 20-cell stack. (b) 3-dimensional features extracted from normal and 5 various faulty states for a 8-cell stack. (c) 3-dimensional features extracted from normal and 4 various faulty states for a 40-cell stack. (d) 3-dimensional features extracted from normal state and 4 various faulty states for a 40-cell stack. The data in normal state (denoted as  $Normal_{time1}$ ,  $Normal_{time2}$ ,  $Normal_{time3}$ ,  $Normal_{time4}$ ) are sampled at different time points.

313 voltages show vary slightly compared with those in normal state. We also  
 314 observe that the wrongly diagnosed data are mostly distributed in the initial  
 315 stage of the fault where the data are located in the transition zone between  
 316 clear normal state and faulty states.

Table 4. Diagnosis accuracy for different faults for different PEMFC stacks

| Fault             | $F_1$  | $F_2$  | $F_3$  | $F_4$   | $F_5$   | $F_6$  | $F_7$  |
|-------------------|--------|--------|--------|---------|---------|--------|--------|
| Stack 1 (20-cell) | 94.01% | 99.21% | -      | -       | -       | -      | -      |
| Stack 2 (8-cell)  | -      | -      | 91.63% | 95.02%  | 100.00% | 89.44% | 99.08% |
| Stack 3 (40-cell) | -      | -      | 93.55% | 100.00% | 99.56%  | 85.14% | -      |

$F_1$ : Membrane drying fault;  $F_2$ : Flooding fault;  $F_3$ : High current pulse fault;  $F_4$ :  
 Cooling water stopping fault;  $F_5$ : High air stoichiometry;  $F_6$ : Low air stoichiometry;  
 $F_7$ : Anode CO poisoning.

### 317 6.2. Online computational complexity

318 Since the diagnosis approach is implemented using the ASIC whose com-  
 319 puting capability and storage capacity are limited compared with a standard  
 320 PC, the online computational complexity of the algorithm needs to be eval-  
 321 uated. In our approach, the needed memories are respectively  $O(ML)$  and  
 322  $O(LS)$  for saving the trained feature extraction and classification models, in  
 323 which  $S$  is the number of support vectors, while the online computing times  
 324 are  $O(ML)$  and  $O(LS)$  for implementing the feature extraction and classifi-  
 325 cation methods. From our test, the occupied memory is less than 200 kb for  
 326 saving the parameters for diagnosis, while the online implementing time of a  
 327 diagnosis cycle can be maintained at the level of 10 ms using the developed



328 ASIC. In our platforms, the sample time was set to 1 s, which means the  
329 diagnosis cycle can be achieved by a large margin. To our knowledge, the  
330 diagnosis cycle obtained in our test could satisfy the requirements for most  
331 fuel cell systems.

### 332 *6.3. Novel fault mode recognition*

333 Conventional classification methods can only be used to recognize the  
334 known faults which have been shown in the training database. When an  
335 example from a new fault mode is treated, it will be diagnosed wrongly into  
336 a known fault class or the normal one. We propose here the modified SVM  
337 and diagnostic rule to overcome this shortcoming. To verify the proposal,  
338 we assumed that a fault is unknown in the training process, and occurs in  
339 the diagnosis stage. Taking the case of a 40-cell stack as example, when  $F_3$ ,  
340  $F_4$ ,  $F_5$ ,  $F_6$  were considered as the unseen fault, the probabilities that they  
341 were successfully recognized as a novel fault mode are respectively 96.77%,  
342 100.00%, 95.36%, 39.86% which are at a high level except the case of  $F_6$ .  
343 This results from the fact that the data in  $F_6$  are too close to the normal  
344 ones. They are mostly classified into the normal state class.

### 345 *6.4. Online adaptation*

346 In consideration of the ageing effects, the performance of the PEMFC  
347 degrades with time. It results that the variables measured in the normal op-  
348 erating state are non-stationary, i.e. the cell voltages decrease to some degree  
349 after a period of time operation. Accordingly, the location of data in normal  
350 state varies in the feature space (Fig. 7(d)). In this case, the initially trained  
351 diagnosis approach may gradually lose its efficiency, i.e., the FAR increases.

352 To maintain the performance, we propose here an online adaptation method.  
353 The online adaptation is realized via incremental learning of the SSM-SVM  
354 classifier. We tested the diagnosis approach with and without online adapta-  
355 tion during long-term operation. The 1st, 2nd, and 3rd tests were carried out  
356 respectively at three different time points (the 20th day, 80th day, 170th day  
357 counting from the beginning of the test). With the initially trained diagnosis  
358 model (without online adaptation), the FARs obtained at the 1st, 2nd, and  
359 3rd tests were respectively 35.5%, 100%, and 100%. This means that more  
360 and more data in normal state were diagnosed as the faulty ones if we did not  
361 modify the initially trained model. By contrast, with our proposed online  
362 adaptation method, the FARs obtained at the 1st, 2nd, and 3rd tests were  
363 respectively 0.25%, 0%, and 0%. The performance of the diagnosis approach  
364 was therefore maintained.

### 365 *6.5. Discussion*

366 The data studied in this paper were acquired from the stacks operated in  
367 nominal steady state. In some applications such as fuel cell vehicles, dynamic  
368 operating conditions should be handled in diagnosis. In these cases, the  
369 correlations of the samples could be considered. To achieve this, data series  
370 instead of single data sample could be treated as the objects for classification  
371 [39].

372 Data-driven diagnosis approach is focused on in this study to coordinate  
373 with the cell voltage measurement. The proposed approach can be combined  
374 with some model-based techniques to handle the system dynamics and to  
375 improve the generalization capability. Hybrid diagnosis approach could be  
376 one promising solution for fuel cell diagnosis [40].

377 The proposed data-driven approach is supposed to be applied jointly with  
378 the developed ASIC. Although in the current commercial PEMFC systems, it  
379 is not easy to measure individual cell voltages. We believe that the proposal  
380 can be interesting for many fuel cell suppliers and can be a potential solution  
381 in their future products.

## 382 **7. Conclusion**

383 In this study, we firstly propose the criteria for online fuel cell online di-  
384 agnosis. To attain these criteria, we experimentally demonstrated an online  
385 fault diagnosis strategy for PEMFC systems. With the specifically designed  
386 ASIC, the proposed diagnosis approach was implemented online to diagnose  
387 multiple faults with respect to several PEMFC stacks. We proposed here to  
388 monitor the individual fuel cell voltages and employ them as the variables for  
389 diagnosis. In contrast to most of the available approaches in which the fuel  
390 cell voltages are assumed to be identical, the inhomogeneity among cells was  
391 utilized and dedicated to fault diagnosis. From a fundamental point of view,  
392 different faults can cause different thermal, fluidic, electrochemical spatial  
393 distributions and these can be reflected by the amplitudes of individual cell  
394 voltages. In this study, it was proved that the individual cell voltages pos-  
395 sess the discriminative information of different health states. The importance  
396 of monitoring every cell voltage, or several of them together, was therefore  
397 stressed. From the diagnostic results of online validation, the diagnosis accu-  
398 racy can be maintained at a high level with respect to different types of fault  
399 and for different fuel cell stacks thanks to the utilization of FDA and SVM  
400 methods. Besides, the capabilities of recognition an unseen faulty mode and

401 online adaptation, which the traditional diagnosis methods are not capable  
402 of handling, were installed into our approach. The efficiency of the ASIC  
403 that we designed here, which is dedicated to precisely measuring and online  
404 implementing the diagnosis algorithm, was validated. The ASIC therefore  
405 promises to be used as a routine component for monitoring fuel cell voltage  
406 and implementing the diagnosis approach we proposed here.

407 Several directions can be interesting on fuel cell diagnosis. First, more  
408 general system model should be built in consideration of different faulty  
409 conditions. Second, more advanced data-based techniques can be applied to  
410 improve the adaptability of the diagnosis methods. Third, the fault diagnosis  
411 should be combined with control strategy to improve the fuel cells' reliability  
412 finally.

413 **References**

- 414 [1] J. Wang, Barriers of scaling-up fuel cells: Cost, durabil-  
415 ity and reliability, *Energy* 80 (2015) 509 – 521. doi:<http://dx.doi.org/10.1016/j.energy.2014.12.007>.  
416 URL <http://www.sciencedirect.com/science/article/pii/S0360544214013644>  
418
- 419 [2] L. Dubau, L. Castanheira, F. Maillard, M. Chatenet, O. Lottin,  
420 G. Maranzana, J. Dillet, A. Lamibrac, J.-C. Perrin, E. Moukheiber,  
421 et al., A review of PEM fuel cell durability: materials degradation, local  
422 heterogeneities of aging and possible mitigation strategies, *Wiley Inter-*  
423 *disciplinary Reviews: Energy and Environment* 3 (6) (2014) 540–560.
- 424 [3] R. Borup, J. Meyers, B. Pivovar, Y. S. Kim, R. Mukundan, N. Garland,  
425 D. Myers, M. Wilson, F. Garzon, D. Wood, et al., Scientific aspects  
426 of polymer electrolyte fuel cell durability and degradation, *Chemical*  
427 *reviews* 107 (10) (2007) 3904–3951.
- 428 [4] Z. Zheng, R. Petrone, M. Péra, D. Hissel, M. Becherif, C. Pianese,  
429 N. Yousfi Steiner, M. Sorrentino, A review on non-model based  
430 diagnosis methodologies for PEM fuel cell stacks and systems, *Inter-*  
431 *national Journal of Hydrogen Energy* 38 (21) (2013) 8914–8926.  
432 doi:[10.1016/j.ijhydene.2013.04.007](http://dx.doi.org/10.1016/j.ijhydene.2013.04.007).  
433 URL <http://linkinghub.elsevier.com/retrieve/pii/S0360319913008550>  
434
- 435 [5] G. Tian, S. Wasterlain, I. Endichi, D. Candusso, F. Harel, X. Fra-

- 436 nois, M.-C. Péra, D. Hissel, J.-M. Kauffmann, Diagnosis meth-  
437 ods dedicated to the localisation of failed cells within PEMFC  
438 stacks, *Journal of Power Sources* 182 (2) (2008) 449 – 461.  
439 doi:<http://dx.doi.org/10.1016/j.jpowsour.2007.12.038>.  
440 URL [http://www.sciencedirect.com/science/article/pii/  
441 S0378775307027061](http://www.sciencedirect.com/science/article/pii/S0378775307027061)
- 442 [6] R. Petrone, Z. Zheng, D. Hissel, M. Pra, C. Pianese, M. Sorrentino,  
443 M. Becherif, N. Yousfi-Steiner, A review on model-based diagnosis  
444 methodologies for PEMFCs, *International Journal of Hydrogen En-  
445 ergy* 38 (17) (2013) 7077 – 7091. doi:[http://dx.doi.org/10.1016/j.  
446 ijhydene.2013.03.106](http://dx.doi.org/10.1016/j.ijhydene.2013.03.106).
- 447 [7] S. X. Ding, *Model-based fault diagnosis techniques*, Vol. 2013, Springer,  
448 2008.
- 449 [8] A. Hernandez, D. Hissel, R. Outbib, Modeling and Fault Diagnosis of  
450 a Polymer Electrolyte Fuel Cell Using Electrical Equivalent Analysis,  
451 *IEEE Transaction on Energy Conversion* 25 (1) (2010) 148–160. doi:  
452 [10.1109/TEC.2009.2016121](http://dx.doi.org/10.1109/TEC.2009.2016121).
- 453 [9] S. de Lira, V. Puig, J. Quevedo, A. Husar, LPV observer de-  
454 sign for PEM fuel cell system: Application to fault detec-  
455 tion, *Journal of Power Sources* 196 (9) (2011) 4298 – 4305.  
456 doi:<http://dx.doi.org/10.1016/j.jpowsour.2010.11.084>.  
457 URL [http://www.sciencedirect.com/science/article/pii/  
458 S0378775310020756](http://www.sciencedirect.com/science/article/pii/S0378775310020756)

- 459 [10] S. Laghrouche, J. Liu, F. Ahmed, M. Harmouche, M. Wack, Adaptive  
460 second-order sliding mode observer-based fault reconstruction for pem  
461 fuel cell air-feed system, *Control Systems Technology*, IEEE Transactions  
462 on 23 (3) (2015) 1098–1109. doi:10.1109/TCST.2014.2361869.
- 463 [11] T. Escobet, D. Feroldi, S. de Lira, V. Puig, J. Quevedo, J. Ri-  
464 era, M. Serra, Model-based fault diagnosis in PEM fuel cell  
465 systems, *Journal of Power Sources* 192 (1) (2009) 216 – 223.  
466 doi:http://dx.doi.org/10.1016/j.jpowsour.2008.12.014.  
467 URL [http://www.sciencedirect.com/science/article/pii/  
468 S0378775308023288](http://www.sciencedirect.com/science/article/pii/S0378775308023288)
- 469 [12] S. Yin, Data-driven design of fault diagnosis systems, Ph.D.  
470 thesis, Universität Duisburg-Essen, Fakultät für Ingenieurwis-  
471 senschaften» Ingenieurwissenschaften-Campus Duisburg» Abteilung  
472 Elektrotechnik und Informationstechnik» Automatisierung und kom-  
473 plexe Systeme (2012).
- 474 [13] D. Hissel, D. Candusso, F. Harel, Fuzzy-Clustering Durability Diagno-  
475 sis of Polymer Electrolyte Fuel Cells Dedicated to Transportation Ap-  
476 plications, *IEEE Transactions on Vehicular Technology* 56 (5) (2007)  
477 2414–2420.
- 478 [14] Z. Li, R. Outbib, S. Giurgea, D. Hissel, Diagnosis for pemfc sys-  
479 tems: A data-driven approach with the capabilities of online adaptation  
480 and novel fault detection, *Industrial Electronics*, IEEE Transactions on  
481 62 (8) (2015) 5164–5174. doi:10.1109/TIE.2015.2418324.

- 482 [15] D. Hissel, M. C. Péra, J. M. Kauffmann, Diagnosis of automotive fuel  
483 cell power generators, *Journal of Power Sources* 128 (2) (2004) 239–246.  
484 doi:<http://dx.doi.org/10.1016/j.jpowsour.2003.10.001>.
- 485 [16] N. Yousfi-Steiner, D. Hissel, P. Moçotéguy, D. Candusso, Diagnosis of  
486 polymer electrolyte fuel cells failure modes (flooding & drying out)  
487 by neural networks modeling, *International Journal of Hydrogen En-  
488 ergy* 36 (4) (2011) 3067–3075. doi:<http://dx.doi.org/10.1016/j.ijhydene.2010.10.077>.
- 490 [17] Y. Vural, D. B. Ingham, M. Pourkashanian, Performance prediction  
491 of a proton exchange membrane fuel cell using the ANFIS model,  
492 *International Journal of Hydrogen Energy* 34 (22) (2009) 9181–9187.  
493 doi:[10.1016/j.ijhydene.2009.08.096](http://dx.doi.org/10.1016/j.ijhydene.2009.08.096).
- 494 [18] J. Hua, J. Li, M. Ouyang, L. Lu, L. Xu, Proton exchange membrane  
495 fuel cell system diagnosis based on the multivariate statistical method,  
496 *International Journal of Hydrogen Energy* (2011) 1–10doi:[10.1016/j.ijhydene.2011.05.075](http://dx.doi.org/10.1016/j.ijhydene.2011.05.075).  
497 URL <http://dx.doi.org/10.1016/j.ijhydene.2011.05.075>
- 499 [19] Z. Zheng, M.-C. Péra, D. Hissel, M. Becherif, K.-S. Ag-  
500 bli, Y. Li, A double-fuzzy diagnostic methodology dedicated  
501 to online fault diagnosis of proton exchange membrane fuel  
502 cell stacks, *Journal of Power Sources* 271 (2014) 570 – 581.  
503 doi:<http://dx.doi.org/10.1016/j.jpowsour.2014.07.157>.  
504 URL [http://www.sciencedirect.com/science/article/pii/  
505 S0378775314012117](http://www.sciencedirect.com/science/article/pii/S0378775314012117)



- 506 [20] L. Alberto, M. Riascos, M. G. Simoes, P. E. Miyagi, On-line fault diag-  
507 nostic system for proton exchange membrane fuel cells, *Journal of Power*  
508 *Sources* 175 (2008) 419–429.
- 509 [21] S. Wasterlain, D. Candusso, F. Harel, X. François, D. Hissel, Diagno-  
510 sis of a fuel cell stack using electrochemical impedance spectroscopy  
511 and bayesian networks, in: *Vehicle Power and Propulsion Conference*  
512 *(VPPC)*, 2010 IEEE, 2010, pp. 1–6. doi:10.1109/VPPC.2010.5729184.
- 513 [22] J. Chen, B. Zhou, Diagnosis of PEM fuel cell stack dynamic behaviors,  
514 *Journal of Power Sources* 177 (1) (2008) 83 – 95. doi:http://dx.doi.  
515 org/10.1016/j.jpowsour.2007.11.038.
- 516 [23] N. Y. Steiner, D. Hissel, P. Moçotéguy, D. Candusso, Non intrusive  
517 diagnosis of polymer electrolyte fuel cells by wavelet packet transform,  
518 *International Journal of Hydrogen Energy* 36 (1) (2011) 740 – 746.  
519 doi:http://dx.doi.org/10.1016/j.ijhydene.2010.10.033.  
520 URL [http://www.sciencedirect.com/science/article/pii/  
521 S0360319910021129](http://www.sciencedirect.com/science/article/pii/S0360319910021129)
- 522 [24] D. Benouioua, D. Candusso, F. Harel, L. Oukhellou, Fuel cell diag-  
523 nosis method based on multifractal analysis of stack voltage signal,  
524 *International Journal of Hydrogen Energy* 39 (5) (2014) 2236 – 2245.  
525 doi:http://dx.doi.org/10.1016/j.ijhydene.2013.11.066.  
526 URL [http://www.sciencedirect.com/science/article/pii/  
527 S0360319913027912](http://www.sciencedirect.com/science/article/pii/S0360319913027912)
- 528 [25] E. Monmasson, M. Cirstea, *FPGA Design Methodology for Industrial*

- 529 Control Systems—A Review, *Industrial Electronics*, *IEEE Transactions*  
530 on 54 (4) (2007) 1824–1842. doi:10.1109/TIE.2007.898281.
- 531 [26] C. Steiger, H. Walder, M. Platzner, Operating systems for reconfigurable  
532 embedded platforms: online scheduling of real-time tasks, *Computers*,  
533 *IEEE Transactions on* 53 (11) (2004) 1393–1407. doi:10.1109/TC.  
534 2004.99.
- 535 [27] P. Rodatz, F. Bchi, C. Onder, L. Guzzella, Operational as-  
536 pects of a large PEFC stack under practical conditions, *Journal of Power Sources* 128 (2) (2004) 208 – 217. doi:http:  
537 //dx.doi.org/10.1016/j.jpowsour.2003.09.060.  
538 URL [http://www.sciencedirect.com/science/article/pii/  
539 S0378775303010085](http://www.sciencedirect.com/science/article/pii/S0378775303010085)  
540
- 541 [28] Z. Li, R. Outbib, S. Giurgea, D. Hissel, Y. Li, Fault detection and iso-  
542 lation for polymer electrolyte membrane fuel cell systems by analyzing  
543 cell voltage generated space, *Applied Energy* 148 (2015) 260 – 272.  
544 doi:http://dx.doi.org/10.1016/j.apenergy.2015.03.076.  
545 URL [http://www.sciencedirect.com/science/article/pii/  
546 S0306261915003682](http://www.sciencedirect.com/science/article/pii/S0306261915003682)
- 547 [29] E. Gerstner, Nobel prize 2007: Fert and grünberg, *Nature Physics* 3 (11)  
548 (2007) 754–754.
- 549 [30] Y. S. Chai, S. Kwon, S. H. Chun, I. Kim, B.-G. Jeon, K. H. Kim, S. Lee,  
550 Electrical control of large magnetization reversal in a helimagnet, *Nature*  
551 *communications* 5.

- 552 [31] Z. Li, R. Outbib, D. Hissel, S. Giurgea, Data-driven diagnosis of PEM  
553 fuel cell: A comparative study, *Control Engineering Practice* 28 (2014)  
554 1–12. doi:10.1016/j.conengprac.2014.02.019.  
555 URL [http://linkinghub.elsevier.com/retrieve/pii/  
556 S0967066114001002](http://linkinghub.elsevier.com/retrieve/pii/S0967066114001002)
- 557 [32] G. McLachlan, *Discriminant analysis and statistical pattern recognition*,  
558 Vol. 544, John Wiley & Sons, 2004.
- 559 [33] J. C. Platt, *Sequential Minimal Optimization : A Fast Algorithm for*  
560 *Training Support Vector Machines*, Technical Report MSR-TR-98-14,  
561 Microsoft Research (1998) 1–21.
- 562 [34] P. Y. Hao, Y. H. Lin, A new multi-class support vector machine with  
563 multi-sphere in the feature space, in: *Proceedings of the 20th interna-*  
564 *tional conference on Industrial, engineering, and other applications of*  
565 *applied intelligent systems, IEA/AIE'07*, Springer-Verlag, Berlin, Hei-  
566 delberg, 2007, pp. 756–765.
- 567 [35] P. Freitas, R. Ferreira, S. Cardoso, F. Cardoso, Magneto-resistive sensors,  
568 *Journal of Physics: Condensed Matter* 19 (16) (2007) 165221.
- 569 [36] M. Pannetier-Lecoecur, C. Fermon, A. Giraud, GMR based integrated  
570 non-contact voltage sensor for fuel cells monitoring, in: *Sensing Technol-*  
571 *ogy (ICST), 2011 Fifth International Conference on*, 2011, pp. 101–105.  
572 doi:10.1109/ICSensT.2011.6136941.
- 573 [37] Z. Li, S. Giurgea, R. Outbib, D. Hissel, Online Diagnosis of PEMFC  
574 by Combining Support Vector Machine and Fluidic Model, *Fuel Cells*

- 575 14 (3) (2014) 448–456. doi:10.1002/fuce.201300197.  
576 URL <http://doi.wiley.com/10.1002/fuce.201300197>
- 577 [38] C. de Beer, P. S. Barendse, P. Pillay, Fuel Cell Condition Monitoring  
578 Using Optimized Broadband Impedance Spectroscopy, *IEEE Transac-*  
579 *tions on Industrial Electronics* 62 (8) (2015) 5306–5316. doi:10.1109/  
580 TIE.2015.2418313.
- 581 [39] Z. Li, R. Outbib, S. Giurgea, D. Hissel, Fault diagnosis for pemfc systems  
582 in consideration of dynamic behaviors and spatial inhomogeneity, *IEEE*  
583 *Transactions on Energy Conversion* (2018) 1–1doi:10.1109/TEC.2018.  
584 2824902.
- 585 [40] Z. Li, R. Outbib, D. Hissel, S. Giurgea, Diagnosis of pemfc by using  
586 data-driven parity space strategy, in: *2014 European Control Conference*  
587 *(ECC)*, 2014, pp. 1268–1273. doi:10.1109/ECC.2014.6862527.